Structure and Function of the Engineered Multicopper Oxidase CueO from Escherichia coli-Deletion of the Methionine-Rich Helical Region Covering the Substrate-Binding Site

Structure and Function of the Engineered Multicopper Oxidase, CueO from *Escherichia coli* — Deletion of the Methionine-Rich Helical Region Covering the Substrate Binding Site —

Kunishige Kataoka, Hirofumi Komori, Yusaku Ueki, Yusuke Konno, Yuji Kamitaka, Shinji Kurose, Seiya Tsujimura, Yoshiki Higuchi, Kenji Kano, Daisuke Seo, Takeshi Sakurai

PII: S0022-2836(07)00969-2
DOI: doi: 10.1016/j.jmb.2007.07.041
Reference: YJMBI 59628

To appear in: *Journal of Molecular Biology*

Received date: 15 May 2007
Revised date: 16 July 2007

Please cite this article as: Kataoka, K., Komori, H., Ueki, Y., Konno, Y., Kamitaka, Y., Kurose, S., Tsujimura, S., Higuchi, Y., Kano, K., Seo, D. & Sakurai, T., Structure and Function of the Engineered Multicopper Oxidase, CueO from *Escherichia coli* — Deletion of the Methionine-Rich Helical Region Covering the Substrate Binding Site —, *Journal of Molecular Biology* (2007), doi: 10.1016/j.jmb.2007.07.041

Structure and Function of the Engineered Multicopper Oxidase, CueO from *Escherichia coli*

— Deletion of the Methionine-Rich Helical Region Covering the Substrate Binding Site —

Kunishige Kataoka[1], Hirofumi Komori[2], Yusaku Ueki[1], Yusuke Konno[1], Yuji Kamitaka[3], Shinji Kurose[1,3], Seiya Tsujimura[3], Yoshiki Higuchi[2], Kenji Kano[3], Daisuke Seo[1] and Takeshi Sakurai[1,*]

[1]Division of Material Sciences, Graduate School of Natural Science and Technology, Kanazawa University, Kakuma, Kanazawa 920-1192, Japan
[2]Graduate School of Life Science, University of Hyogo, 3-2-1 Kouto, Kamigori-cho, Ako-gun, Hyogo 678-1297, Japan
[3]Division of Applied Life Sciences, Graduate School of Agriculture, Kyoto University, Kitashirakawa Oiwake-cho, Sakyo-ku, Kyoto 606-8502, Japan

*Corresponding author

Running Title: Engineered Multicopper Oxidase CueO

Abbreviations used: MCO, multicopper oxidase; ABTS, 2,2'-azino-bis(3-ethylbenzothiazoline-6-sulfonic acid); *p*-PD, *p*-phenylenediamine; 2,6-DMP, 2,6-dimethoxyphenol; rCu, regulatory Cu; rCueO, recombinant CueO; IMAC, immobilized metal ion affinity chromatography; PCR, polymerase chain reaction; CD, circular dichroism; EPR, electron paramagnetic resonance; DPPH, 1,1-diphenyl-2-picrylhydrazyl; NHE, normal hydrogen electrode; SUR, structurally unconserved region.

E- mail address of the corresponding author: ts0513@kenroku.kanazawa-u.ac.jp

CueO is a multicopper oxidase involved in the homeostasis of Cu in *Escherichia coli*, and functions as the sole cupric oxidase ever found. Differing from other multicopper oxidases, the substrate-binding site of CueO is deeply buried under a methionine-rich helical region including α-helices 5, 6, and 7 that interfere the access of organic substrates. We deleted this region, Pro357-His406 and replaced it with a Gly-Gly linker. Crystal structures of the truncated mutant in the presence and absence of excess Cu(II) indicated that the scaffold of the CueO molecule and the metal binding sites were reserved in comparison with those of CueO. In addition, the high thermostability of the protein molecule and spectroscopic and magnetic properties due to the four Cu centers were also conserved after the truncation. As for functions, the cuprous oxidase activity of the mutant was reduced to ca. 10% of that of recombinant CueO owning to the decrease in the affinity of the labile Cu site for Cu(I) ions, although activities for laccase substrates such as 2,2'-azino-bis(3-ethylbenzothiazoline-6-sulfonic acid), *p*-phenylenediamine, and 2,6-dimethoxyphenol increased due to the changes in accessibilities of these organic substrates towards the type I Cu site. The present engineering of CueO indicates that the methionine-rich α-helices function as a barrier to interfere with the access of bulky organic substrates to provide CueO with the specificity as cuprous oxidase.

Keywords: CueO; multicopper oxidase; homeostasis; truncated mutant; X-ray crystal structure

Introduction

Multicopper oxidases (MCOs) are enzymes containing a multiple copper center to catalyze the oxidation of a variety of substrates such as polyphenols, aromatic polyamines, L-ascorbate, and metal ions concomitantly with the four-electron reduction of dioxygen to water.[1-5] Laccase, the largest subfamily of MCOs, shows multiple functions including lignin degradation, pigmentation, and pathogenesis in fungi as well as lignin biosynthesis and wound healing in plants.[6-10] Therefore, structures and functions of new MCOs such as *Escherichia coli* CueO (formerly called YacK)[11-13] and *Bacillus subtilis* CotA,[14,15] have been discussed in comparison with those of laccase.

CueO is a 53.4-kDa periplasmic protein involved in the Cu efflux system, together with CopA, the P-type ATPase.[16] CueO is responsible for the oxidation of cuprous ion to less toxic cupric ion and the oxidation of enterobactin to prevent the copper-catalyzed Fenton reaction so as not to sequester iron from the environment.[17,18] CueO also catalyzes the oxidation of organic compounds including 2,2'-azino-bis(3-ethylbenzothiazoline-6-sulfonic acid) (ABTS), *p*-phenylenediamine (*p*-PD), and 2,6-dimethoxyphenol (2,6-DMP). Oxidase activities of CueO toward these substrates are considerably low, but are fairly enhanced in the presence of an excess Cu(II) ions.[11,12] That is, the enzymatic activity of CueO is regulated by Cu ions in *E. coli*.

Crystal structures of eleven MCOs have been determined; ascorbate oxidase,[19] ceruloplasmin, [20] five fungal laccases,[21-26] Fet3p,[27] CueO,[28] CotA,[29] and phenoxazinone synthase.[30] The archetypal MCO consists of about 500 amino acid residues and has the three domains, each of which basically has an eight-stranded Greek key β-barrel fold (cupredoxin fold).[31] Cupredoxins are the family of small blue copper (type I Cu) proteins ($M_r \approx 14$ kDa) characterized by the very intense Cys(S^-)→Cu(II) charge transfer transition band in the visible spectrum ($\lambda_{max} \approx 600$ nm, $\varepsilon \approx 5{,}000$), high redox potential (+180 ~ +680 mV) and the narrow hyperfine splitting in the EPR spectrum ($A_Z \approx 4$~8×10^{-3} cm^{-1}).[32] Only the C-terminal cupredoxin domain (domain 3) of MCO has a type I Cu site, which transfers electrons from the substrate to the trinuclear Cu center composed of a type II Cu and a pair of type III Cu atoms located at the interface of domains 1 and 3 and reduces dioxygen to two

water molecules.

According to the structures of multicopper oxidases,[19-27,29,30] the type I Cu site is positioned at the bottom of the widely opened substrate-binding cleft and an imidazole edge of the type I Cu ligand is exposed to solvent water. Whereas, the type I Cu site consisting of His443, Cys500, His505, and Met510 in CueO is completely isolated from the solvent water by the methionine-rich insertion sequence (amino acid residues 355–400 of which fourteen residues are Met) including α-helices 5, 6, and 7. In particular, the longest helix 5 (amino acid residues 356–371), which includes seven methionine residues, interferes with the access of organic substrates to the type I Cu site (Figure 1). Beneath helix 5, the labile regulatory Cu (rCu) binding site comprised of Met355, Asp360 (being present in helix 5), Asp439, and Met441 is located only 7.5 Å apart from the type I Cu site. Both Cu sites are connected with a hydrogen bond between OD2 of Asp439 and NE2 of His443.[33] The rCu site is the site to bind the substrate Cu(I) ion, although the crystal structure analysis of Cu(II)-soaked CueO revealed that a Cu(II) ion was bound at this site. The activities of CueO toward organic substrates are enhanced in the presence of excess Cu(II) because rCu functions as the mediator of electron transfer between substrates and type I Cu.[33]

Several different types of recombinant CueO (rCueO) have been expressed to date such as Strep-tag attached rCueO using the vector pASK-IBA3 (IBA) and rCueO without an attached peptide using a specifically controlled expression vector.[11,12] We constructed a new expression system of CueO with 6xHis tag at the C-terminus (hereafter all recombinant CueOs are abbreviated as rCueO) suitable for the purification with the immobilized metal ion affinity chromatography (IMAC). The native CueO, which might be induced by excess Cu supplemented in culture medium, can be excluded by performing IMAC. By using this expression system we preliminary prepared a variant of CueO (Δα5-7 CueO), in which 50 amino acid residues (Pro357–His406 of which thirteen residues are Met) including α-helices 5, 6, and 7 (colored red in Figure 1), and 23 residues spanning between helices 6 and 7 as an unstructured loop (amino acid residues 380–402) were deleted from rCueO, and a Gly–Gly linker to connect the anti-parallel β-strands was inserted so as not to deform the CueO scaffold.[34] In the present report, we determined the crystal structure of Δα5-7 CueO and studied how the function

of this first extensively engineered MCO was modified without changing the scaffold structure and spectroscopic properties.

Results

Structure of Δα5-7 CueO

The crystal structure of Δα5-7 CueO has been determined at 1.81 Å resolution. The asymmetric unit contains two Δα5-7 CueO molecules (molecule A and molecule B), which are related by a pseudo-twofold symmetry (Supplementary Data Fig. 1). Both molecules form a head-to-head interaction at the surface region exposed by deletion of α–helices 5-7, although Δα5-7 CueO is monomeric in solution as evidenced by gel-filtration chromatography (not shown). There is a nitrate ion which probably originated from the crystallization precipitant at the interface between molecule A and molecule B. The overall fold of both molecules is almost identical to that of rCueO[28,33] (The root mean square distance for 435 Cα atoms of molecule A of Δα5-7 CueO with rCueO is 0.39 Å) except for the loop region between domains 2 and 3 (> 2 Å) (Figure 2 and Supplementary Data Fig. 2). Figure 3 shows the overall structure of Δα5-7 CueO (molecule A) comprised of three domains as rCueO and other MCOs.[19-30] Molecule A and molecule B have essentially the same fold, although the C-terminal 6xHis-tag region of the molecule B is disordered (Supplementary Data Fig. 3). The structural discrepancy at this region between Δα5-7 CueO and rCueO may be caused by the crystal packing interaction.

The structures of the active sites (Figure 4, Table 2) are also almost identical to those of rCueO[28,33] except for the bridging group between type III Cu's. In the present Δα5-7 CueO, an oxygen atom has been satisfactorily refined as a bridging species with an acceptable temperature factor at the trinuclear Cu center. On the other hand, a Cl^- ion bridged between type III Cu's in rCueO, [28,33] although the OH^- bridged form of rCueO has been reported very recently.[35] The angle around oxygen, Cu2 (type III)—O—Cu3 (type III), of molecule A (B) in the structure of Δα5-7 CueO is 149.8°

(146.9°), while that around Cl^-, Cu2 (type III)—Cl—Cu3 (type III), in the structure of rCueO has been reported as 169.3°. Bridging of the naturally occurring group (OH^- or O^{2-}) afforded the bond angle similar to values reported for other MCOs.[19-30] The bonding distances of Cu (type III)—O in molecule A (B) were refined to 1.96 (1.96) for Cu2 and 1.97 (1.95) Å for Cu3, respectively, while those of Cu (type III)—Cl were 2.29 (Cu2) and 2.43 Å (Cu3). In addition, the distance of Cu (type II)—O (H_2O or OH^-) has been also reduced from 2.96 Å in rCueO to 2.49 (2.52) Å for molecule A (B) in Δα5-7 CueO, although it is not clear whether the discrepancy was induced directly by the deprotonation from the coordinated water molecule or indirectly by the difference in the bridging species between type III Cu atoms. The oxidation state of all Cu atoms is divalent as evidenced by spectroscopies (*vide infra*). The overlapped structures around the fifth copper (rCu) binding site of rCueO and Δα5-7 CueO (Figure 4 and refs. 28 (PDB accession code 1KV7) and 35 (2FQF)) indicate that the spatial arrangement of the side chains of Asp439 and Met441 changes upon the binding of a Cu(II) ion at this site.

The crystal structure of Δα5-7 CueO soaked with 10 mM Cu(II) for several sec has been determined at 1.50 Å (Supplementary Data Fig. 2 and Fig. 3B). Soaking of Cu(II) in the crystal of Δα5-7 CueO did not affect the overall folding of the protein molecule except for the conformational changes around the C-terminal 6xHis-tag region caused by the coordination of exogenous Cu ions. The anomalous difference map of Cu-soaked Δα5-7 CueO showed clear density peaks corresponding to the exogenous two Cu ions positioned at the interface of molecule A and molecule B. One Cu is coordinated by His518 (molecule A), His518 (molecule B) and His520 (molecule B), and the other one by Glu110 (molecule A), His494 (molecule A), His519 (molecule B) and His522 (molecule B). As mentioned above, the C-terminal region of molecule B is disordered in the structure of Δα5-7 CueO without additional Cu ions. On the contrary, this region of molecule A is disordered in Cu-soaked Δα5-7 CueO. No electron density, which can be assigned as Cu, was found at the rCu-binding site in the structure of Δα5-7 CueO even with excess Cu.

The region at the interface of CueO was flattened after the truncation. Although the presence of a deep substrate-binding pocket is not recognized, it is expected

that Δα5–7 CueO shows the increased activities for organic substrates by removing the bulky region (*vide infra*). Since the rCu site without Asp360 is now exposed to solvent, it is also expected that its role as the mediator of electron transfer in the presence of excess Cu(II) is modified.

Spectroscopic and electrochemical properties of Δα5-7 CueO

The electronic absorption spectrum of Δα5-7 CueO is illustrated in Figure 5A together with that of rCueO. The truncated mutant showed intense blue color due to the charge transfer, S^-_π(Cys) → Cu(II), originating in type I Cu at 612 nm (ε ≈ 6,000 at pH 6.0) similarly to rCueO. The shoulder at about 330 nm (ε ≈ 5,000 at pH 6.0) due to the charge transfer, OH^- → Cu(II) (type III) was also observed for both rCueO and Δα5-7 CueO.

The circular dichroism (CD) spectral features of rCueO and Δα5-7 CueO were also highly similar over wavelengths 300-800 nm, affording the charge transfer bands, OH^- → Cu(II) (type III) at 330 nm (-), N(His) → Cu(II) at 440 nm (-), S^-_σ(Cys) → Cu(II) at ca. 520 nm (+, shoulder), S^-_π(Cys) → Cu(II) at 580 nm (+), and d-d bands at 745 nm (-) (Figure 5A).

Both signals due to type I and type II Cu ions were observed in the EPR spectrum of Δα5-7 CueO (solid line in Figure 5B): the spin Hamiltonian parameters were g_{II} = 2.24 and A_{II} = 6.7 x 10^{-3} cm^{-1} for type I Cu and g_{II} = 2.24 and A_{II} = 19.0 x 10^{-3} cm^{-1} for type II Cu. These spin Hamiltonian parameters were the same with those of the present rCueO (dotted line) and those of rCueO in lit. 18, although those of type II Cu in rCueO have been reported to be g_{II} = 2.26 and A_{II} = 15.2 x 10^{-3} cm^{-1} in ref. 11. This discrepancy might originate in the difference in the assignments of the type II Cu signal (an extra Cu might be present in the case of ref. 11) or the indirect effect due to the bridging of Cl^- between type III Cus (*vide infra*). The total amount of the EPR-detectable Cu^{2+} was 1.9 per protein molecule, ensuring that type I Cu and type II Cu ions were fully oxidized and type III Cu ions were antiferromagnetically coupled. All the spectral features above indicate that the electronic structure of the Cu-binding sites in Δα5-7 CueO was not affected at all by the truncation of the helical region.

rCueO did not give clear redox waves in the cyclic voltammogram, although the $E°'$ value due to type I Cu could be estimated to be +0.36 V vs. normal hydrogen electrode (NHE) at pH 6.0 by successive measurements using an Au electrode modified with various promoters (Figure 6 and data not shown). In contrast, Δα5-7 CueO gave unequivocal quasi-reversible electron transfer responses, $E°' = +0.37$ mV with a peak-to-peak separation of $\Delta E_p = 87$ mV at pH 6.0, indicating that the electric communication between electrode and protein molecule became much easier due to the truncation without any change in the redox potential of type I Cu (experimental error is ca. 0.01 V).

Effect of temperature and pH on the activities and stability of Δα5-7 CueO

Incubations of rCueO and Δα5-7 CueO in 100 mM potassium phosphate buffer, pH 6.0, over the range of 30-75°C, showed that their oxidation activities for *p*-PD increased continuously with increasing temperature, thus the optimal temperatures of both rCueO and Δα5-7 CueO were found to be higher than 75°C. As for thermostabilities, both enzymes retained full activity following incubation at 50°C for 30 min, whereas about 50% activity was lost by incubation at 60°C. The half-inactivation time of Δα5-7 CueO, $t_{1/2} = 28$ min at 60°C, was slightly shorter than that of rCueO, $t_{1/2} = 38$ min (Supplementary Data Fig. 4). All these findings indicate that Δα5-7 CueO conserved high thermostability comparable to rCueO in spite of the deletion of 50 amino acids.

pH dependences of the oxidase activity of rCueO and Δα5-7 CueO for *p*-PD were determined (pH 2-12). The optimum pH of Δα5-7 CueO was 7.5, slightly lower than that of rCueO (pH 8.0). The stability of Δα5-7 CueO decreased sparingly compared to rCueO over the pH range of 6 to 11 by incubation at 25°C for 60 min in the same buffer (data not shown).

Catalytic properties of Δα5-7 CueO

The oxidations of 2,6-DMP by rCueO and Δα5-7 CueO in the presence of various concentrations of Cu(II) ion were studied in order to determine the affinity of the rCu site for Cu(II) (Supplementary

Data Fig. 5). The K_m value of Δα5-7 CueO was determined to be 0.77 mM, five-times higher than that of rCueO (K_m = 0.14 mM), while the V_{max} values were the same (34 U/mg).

The substrate specificity of Δα5-7 CueO was examined for the oxidation of Cu(I), Fe(II), ABTS, *p*-PD, and some phenolic substrates in comparison with that of rCueO (Table 3). The oxidase activities were measured in the presence and absence of excess Cu(II), 1 mM for rCueO and 10 mM for Δα5-7 CueO. The amount of Cu(II) added was determined based on the K_m values to ensure full occupation of the rCu site. The cuprous oxidase activity of Δα5-7 CueO was reduced to ca. 10% of that of rCueO owning to the decrease in the affinity of the rCu site for Cu(II) ions. The K_m values for Cu(I) were not obtained because inhibition occurred at > 0.1 mM Cu(I) and did not reach the saturation condition. The activity of Δα5-7 CueO with Fe(II) was almost the same as that of rCueO.

The truncated mutant demonstrated about 30-times and 10-times higher activities for ABTS and *p*-PD, respectively, contrary to those of rCueO in the absence of exogenous Cu(II), while the activities in the presence of excess Cu(II) were comparable to those of rCueO. On the other hand, Δα5-7 CueO exhibited no reactivity with phenolic substrates such as 2,6-DMP, catechol, or guaiacol in the absence of Cu(II) ion as in the case of rCueO. However, when excess Cu(II) was present, Δα5-7 CueO showed higher activity with catechol than rCueO. Oxidizing activities with guaiacol and syringaldazine newly emerged in Δα5-7 CueO. Therefore, the effect of the deletion on oxidase activities appears to differ for each substrate depending on the affinity for them.

Table 4 summarizes the steady-state kinetic parameters of rCueO and Δα5-7 CueO for typical laccase substrates, ABTS, *p*-PD, and 2,6-DMP. In the oxidation of ABTS by Δα5-7 CueO, the K_m value was double that of rCueO in both the presence and absence of excess Cu(II) (11-12 mM). rCueO exhibited a dramatic increase in the V_{max} values for ABTS, 1.1 to 34 U/mg on addition of excess Cu(II). In contrast, Δα5-7 CueO showed V_{max} = 46 U/mg even in the absence of excess Cu(II). The K_m value of Δα5-7 CueO for *p*-PD decreased to 25% of that of rCueO and the V_{max} value increased twofold as a result of the helix deletion as well. On the other hand, no significant change occurred in the K_m and V_{max} values for the oxidation of 2,6-DMP.

Discussion

Crystal structure of Δα5−7 CueO (Figures 2 and 3) indicated that the folding of the domain 3 core and the inter-domain interactions were not disordered by the deletion of the 50 amino acid residues, since the β–barrel structure was rigid. The linker dipeptide adequately formed a short reverse turn to connect the anti-parallel ends of the β-strands as expected. In the packing of the Δα5-7 CueO molecules, the interface of molecule A and molecule B is mainly formed with the region exposed by the deletion of α-helix 5 from rCueO. The eight conserved segments (β strands) comprising the core structure of each cupredoxin domain of CueO are connected by seven structurally unconserved regions (SURs).[30] The region deleted from CueO, α-helices 5, 6 and 7, and the disordered loop between α-helices 6 and 7, corresponds to the variant region of the cupredoxin superfamily (SUR1 in Figure 1B). Together with SUR4 and SUR7, this region forms the substrate-binding site in MCOs such as ascorbate oxidase[18] and the interface region in a structural variant of MCO family, Cu nitrite reductase, to interact with the redox couple, pseudoazurin.[36,37]

The maintenance of the scaffold structure of CueO in the truncated mutant led to the preserved high thermostability (Supplementary Data Fig. 4). Furthermore, the content of four Cu ions and all spectroscopic features were the same with those of rCueO (Figure 5) because type I, II, and III Cu sites were not modified by the truncation. Therefore, only the initial stage of the reaction of MCO, the access of substrate towards the protein surface and the following electron transfer to type I Cu site are affected by the truncation.

The improvement in the electrochemical response without any change in the redox potential of type I Cu (Figure 6) will be derived from that the distance from the protein surface to type I Cu is shortened about 3-5 Å. The change in the electrostatic potentials of the protein surface before and after the truncation (Supplementary Data Fig. 6 viewed from the north side) indicates that the area of the negative potential decreased and this might have also led to the better electrochemical communication of Δα5−7 CueO with the electrode.

The rCu-binding site comprised of Met355, Asp360, Asp439, and Met441 in rCueO is positioned

beneath α-helix 5 (above the type I Cu site). Since one of the four ligand residues, Asp360, was involved in the deleted α-helix 5, the binding affinity of the rCu site for Cu(II) was lowered by the truncation (the K_m value changed from 0.14 to 0.77 mM (Supplemental Data Fig. 5)), and Cu(II) was not bound at the rCu site after the soaking of 10 mM Cu(II). Instead, two Cu ions were found at the interface of molecule A and molecule B involving the 6xHis-tag sequences (Supplementary Data Fig. 2B). It is considered that the binding of two Cu ions takes place only in the crystalline form of Δα5–7 CueO containing 6xHis-tag in the C terminus. These Cu ions cannot affect the enzyme activities in the presence of excess Cu(II) (Tables 3 and 4), because Cys500Ser mutant, in which type I Cu site is vacant but the trinuclear Cu center is still able to react with dioxygen, shows no enzyme activity regardless of the presence of excess Cu(II) (unpublished data).

The dramatic decrease in the cuprous oxidase activity from 187 to 21 U/mg was derived from the truncation of Asp360 (Table 3) leading to a decrease in the affinity for Cu(I), although the exact K_m value could not be determined because of inhibition at high Cu(I) concentrations. In addition, the loss of the cage effect of the region covering the rCu site and the deletion of the thirteen Met residues frequently found in metal trafficking systems[38] might have also contributed to the decrease in the cuprous oxidase activity. In contrast, the change in ferroxidase activity was not significant (from 0.91 to 0.70 U/mg), suggesting that the affinity for Fe(II) was not greatly lowered by the truncation or Fe(II) was not bound at the rCu site. The increases in the oxidizing activity with ABTS and *p*-PD by ca. 30 and 10 times, respectively, and the newly emerged activity for syringaldazine indicates that the truncation favored the access of these organic substrates to the region near the type I Cu site, as was also indicated by changes in the K_m and V_{max} values (Table 4). Nevertheless, 2,6-DMP, catechol, and guaiacol were still not oxidized by Δα5-7 CueO, suggesting that other factors might also influence the specific activity change for these organic substrates, such as their low affinities towards the "flattened" surface of the Δα5-7 CueO molecule. Namely, the absence of a clevis to accommodate organic substrates did not lead to the increases in the affinities for organic substrates (Table 4).

In the case of laccase, the imidazole edge of one of the His residues coordinating type I Cu is exposed to solvent water on the wall near the bottom of the substrate binding pocket, functioning as

the effective pathway of electron transfer between substrate and type I Cu.[19,22,29] However, α-helix 4 corresponding to SUR1 in domain 2 isolates this amino acid (His443) from solvent water (Figures 3 and 4), interfering its direct interaction with organic substrates.

According to the docking structures of an inducer or substrate with laccase and CotA, an Asp residue located near to type I Cu site assists the binding of the substrate and abstraction of a proton form it.[22,29] The corresponding amino acid residue in CueO is Asp439 as one of the ligands to rCu. The crystal structure of Δα5-7 CueO unequivocally indicates that the carboxy group in the side chain of this amino acid is exposed to solvent after the truncation, although it is still hydrogen-bonded with His443 for type I Cu (Figure 4). Thus, it appears that Asp439 does not function in the binding of phenolic substrates such as 2,6-DMP and catechol and/or the deprotonation from them (Table 3).

All modifications on enzyme activities as above are in the absence of excess Cu(II) ion. The extent of the decrease in the cuprous oxidase activity of Δα5-7 CueO was practically the same regardless of the presence of rCu (Table 3), because Cu(II) formed as the product possibly functioned as the mediator of electron transfer between Cu(I) in the bulk water and type I Cu.[11,12] The increase in the ferroxidase activities of rCueO and Δα5-7 CueO in the presence of rCu was also derived from the function of rCu as the mediator of electron transfer between substrate and type I Cu. Oxidizing activities of Δα5-7 CueO for ABTS and *p*-PD, which increased ca. 10-30 times even in the absence of rCu, increased further in the presence of rCu (Table 3). The analogous K_m values for the oxidation of ABTS by both rCueO and Δα5-7 CueO, regardless of the presence and absence of excess Cu (Table 4), indicate that the access of ABTS towards the protein molecule may not involve the rCu site (Soaking of ABTS did not give the docked structure). On the other hand, the emergences of the 2,6-DMP and catechol oxidase activities of both rCueO and Δα5-7 CueO in the presence of rCu (Table 3) might be due to this Cu as the mediator of electron transfer. Increases in the redox potential of type I Cu in the CotA mutants, Met502Leu/Phe[15] and the decrease in the redox potential of type I Cu in the

bilirubin oxidase mutant, Met467Gln[4], led to the decreases in the enzyme activities, but the redox potential of type I Cu did not change by the present deletion (Figure 6). Therefore, the increase or the emergence of the oxidizing activities of Δα5-7 CueO with catechol, guaiacol and syringaldazine in the presence of rCu might be accounted for by that these organic substances interacted with the region including the rCu site.

These kinetic results evidenced that the deletion of the 50-amino acid residues facilitated the access of organic substrates to the exposed rCu site directly or to the type I Cu site indirectly. Therefore, we can conclude that the presence of the unique region covering the rCu site is the molecular architecture of CueO to produce the specificity for Cu(I). The facile electron transfer between the electrode and the type I Cu site in Δα5-7 CueO (Figure 6) also supports that the truncated region functions as a barrier to organic substrates. The catalytic efficiency (V_{max}/K_m) for *p*-PD at pH7.5 was remarkably increased by the truncation, from 0.15 to 1.2 U/mg/mM, a value comparable to bilirubin oxidase (8.5 U/mg/mM at pH 6.5)[39] and laccase from *Lentinula edodes* (2.8 U/mg/mM at pH 5.0).[40] Δα5-7 CueO is the first example of the successful modification of the function of MCO to a large extent and extensive engineerings of the protein molecule are expected to lead to the creations of novel functions.

Materials and Methods

Materials

The vector pUC18 (Takara Biochemicals) was used for DNA cloning and recombinant protein expression. *E. coli* JM109 was used for gene manipulations, and *E. coli* BL21 (Novagen) for protein expression. *Taq* DNA polymerase, restriction endonucleases, and other modifying enzymes were obtained from Takara Biochemicals and TOYOBO. Oligonucleotides were purchased from BEX (Japan). All other chemicals were of analytical grade.

Protein expression and purification of the recombinant CueO

The 1.6-kbp gene fragment consisting of the structural gene of CueO (*yacK*), 6xHis-tag, *Eco*RI linker, and *Bam*HI linker was amplified by PCR using *E. coli* JM109 genomic DNA as the template and two oligonucleotides (P1, 5'-GAAGAATTCATGCAACGTCGTGATTTCTTAAAAT-3' coding for the N-terminal region of CueO and the *Eco*RI digestion sequence (underlined); P2, 5'-TTGGATCCTTAATGATGATGATGATGATGGCCTACCGTAAACCCTAAC-3' coding for the 6xHis-tag attached to the C-terminal region of CueO, termination codon and the *Bam*HI digestion sequence (underlined)). The PCR products were digested with *Eco*RI and *Bam*HI and subcloned into pUC18 digested with *Eco*RI and *Bam*HI to yield pUCCueO. The inserted gene was analyzed by DNA sequencing.

E. coli BL21 cells containing pUCCueO were grown in liquid LB medium supplemented with 1 mM $CuCl_2$, 0.5 mM IPTG, and 100 mg/ml sodium ampicillin for 12 h at 32°C with shaking. Periplasmic fractions of the cells were obtained by cold osmotic shock as follows. *E. coli* cells to express rCueO were harvested by centrifugation (10,000 x *g* for 10 min) and washed with cold 10 mM Tris-HCl buffer, pH 8.0 (the same volume as the culture medium). The washed cells were suspended in a 20% sucrose solution buffered at pH 8.0 with 100 mM Tris-HCl (25%-volume of the medium) and left on ice for 10 min. After centrifugation, the cells were resuspended with ice-cold water (20%-volume of the medium) containing Complete protease inhibitor cocktail (Roche). The cell suspension was further left on ice for 10 min, and then centrifuged at 10,000 x *g* for 20 min. The supernatant was centrifuged again (90,000 x *g* for 30 min) to obtain the crude periplasmic fraction.

The periplasmic fraction was applied directly to a BD TALON cobalt affinity resin (BD Bioscience) column equilibrated with 50 mM potassium phosphate buffer (pH 7.0) containing 300 mM NaCl. After washing the column with the same buffer, rCueO was eluted with the same buffer supplemented with 150 mM imidazole. The recombinant protein was further purified using an UnoQ-12 column (BIO-RAD) equilibrated with 20 mM Tris-HCl (pH 8.0). The recombinant protein was eluted with a linear gradient of NaCl (0 – 1.0 M) in the same buffer. The protein purity was

confirmed by SDS-polyacrylamide gel electrophoresis.

The total Cu content in rCueO was 3.6 per protein molecule as determined by atomic absorption spectroscopy (experimental error in determining the Cu content was ca. 10%), indicating that four intrinsic Cu ions were incorporated into the active site. The Cu content did not increase after the action of Cu(II) under air or Cu(I) under Ar and dialysis against the buffer solution, ensuring that apo-protein was not present.

Protein engineering of Δα5-7 CueO

The mutagenesis to delete 50 residues (Pro357–His406) including α-helices 5, 6, 7, and the loop between helices 6 and 7 was performed by a two-step PCR method[41,42] using pUCCueO as the template and sense and antisense mutagenic oligonucleotides designed to lack the amino acid codons from Pro357 to His406 but to insert the codons for Gly-Gly (underlined) as a linker to connect between Asp356 and Ala407 (P3, 5'-GTTGGCACCACCGTCCATGGAGAGTTGCAGCTTGCGTAC-3'; P4, 5'-CTCTCCATGGACGGTGGTGCCAACAAAATCAACGGTC-3'). After the second PCR using primers P1 and P2, the amplified fragment was digested with *Eco*RI and *Bam*HI and cloned into pUC18 to yield pUCCueO-Δα5-7. The CueO mutant gene was sequenced and expressed in *E. coli* BL21 to purify the mutant protein. Δα5–7 CueO was isolated similarly to rCueO. The *m/z* value of Δα5-7 CueO was determined to be 48,725 (the calculated value of apo Δα5–7 CueO is 48,652) from MALDI-TOF mass spectroscopy, during which a portion of Cu were lost by ionization, although the atomic absorption spectroscopy indicated the presence of 3.7 Cu atoms in a protein molecule.

Crystallization, structure determination and refinement

Crystallization was performed by the sitting-drop vapor-diffusion method at 20°C using equal volumes of protein (2 μl) and precipitant (2 μl) solutions consisting 16% polyethylene glycol 3350, 160 mM potassium nitrate and 20% glycerol. Crystals appeared after a few days and grew to approximate dimensions of around 0.2 × 0.2 × 0.1 mm within one week. X-ray diffraction data sets were collected at 100 K freezing in a nitrogen cold stream. The crystal diffracts to 1.81 Å resolution using a rotating anode source (RIGAKU RA-mirco7). The crystal-to-detector distance was maintained at 120 mm with an oscillation range per image of 0.5°, covering a total oscillation range of 180°. Determination of the unit-cell parameters and integration of reflections were performed using the program MOSFLM.[43] The space group is P_1 and the unit-cell parameters were determined to be a = 49.98 Å, b = 50.95 Å, c = 86.05 Å, α = 83.2º, β = 90.8º and γ = 66.7º. The Δα5-7 CueO with exogenous copper ion was prepared by soaking crystal into reservoir solution containing 10 mM $CuSO_4$. X-ray diffraction data sets of copper soaked Δα5-7 CueO were collected at a synchrotron source (beam line BL38B1 SPring-8). The structure was determined by molecular replacement method with the program MOLREP,[44] using the structure of rCueO as a starting model. A simulated annealing refinement was carried out with CNS.[45] Alternate rounds of model-building and refinement were carried out for further completion of the model using $2F_o$-F_c and F_o-F_c maps with the interactive molecular graphics program COOT.[46] The progress of the TLS refinement with REFMAC[47] was assessed by monitoring the R-free value for 5% of the total reflections excluded from the minimization.[48] The final model consists of molecule A and molecule B of Δα5-7 CueO and a nitrate ion from the crystallization buffer binds to their interface, which is produced by the deletion of α–helix 5 to α–helix 7. Data collection and refinement statistics are in Table 1. Model geometry was analyzed with program PROCHECK[49] and no residues were found in the disallowed region of the Ramachandran plot. The figures were prepared by programs PyMOL (pymol.sourceforge.net),[50] MOLSCRIPT,[51] RASTER3D[52] and MolFeat (FiatLux).

Spectral and electrochemical measurements

Absorption spectra were measured on JASCO Ubest-50 and JASCO V-560 spectrometers. CD spectra were measured on a JASCO J-500C spectropolarimeter. X-band EPR spectra were recorded on a JEOL JES-RE1X spectrometer at 77 K. The total amount of EPR-detectable Cu^{2+} was determined by the double integration method using Cu-EDTA as the standard. Signal intensities due to the differences in tuning conditions were calibrated with 1,1-diphenyl-2-picrylhydrazyl (DPPH) as an external standard. The content of copper per protein molecule was determined on a Varian SpectrAA-50 atomic absorption spectrometer. Cyclic voltammetric measurements were carried out using a Bioanalytical Systems (BAS) Model CV-50W voltammetric analyzer with a three-electrode system consisting of a Ag/AgCl reference electrode, a platinum plate counter electrode, and a thioglycolate-modified gold working electrode under an Ar atmosphere at 25°C.

Kinetic analysis

Oxidase activities of rCueO and Δα5-7 CueO were determined by the absorption increases of the oxidized products or by the amount of consumed dioxygen detected using a Clark-type oxygen electrode connected to an Oxygraph 9 DO monitor (Central Kagaku) at 25°C. The oxidation reactions of ABTS, 2,6-DMP, *p*-PD, $FeSO_4{\cdot}(NH_4)_2SO_4{\cdot}6H_2O$ (Mohr's salt), catechol (1,2-benzenediol), guaiacol (2-methoxyphenol), and syringaldazine were followed by the initial absorption changes at 420 nm (ε = 36,000 $M^{-1}cm^{-1}$), 477 nm (ε = 14,800 $M^{-1}cm^{-1}$), 487 nm (ε = 14,700 $M^{-1}cm^{-1}$), 315 nm (ε = 2,200 $M^{-1}cm^{-1}$), 450 nm (ε = 2,000 $M^{-1}cm^{-1}$), 436 nm (ε = 6,600 $M^{-1}cm^{-1}$), and 525 nm (ε = 65,000 $M^{-1}cm^{-1}$), respectively, in 0.1 M acetate buffer (pH 5.5). For the determinations of cuprous oxidase activity, $[Cu(I)(MeCN)_4]PF_6$ (Sigma) was used as described by Singh *et al*.[17] Inactivations of rCueO and Δα5-7 CueO were followed for 2h at 60°C. Enzyme activities depending on pH were measured in 100 mM Britton-Robinson buffer.

Protein Data Bank accession codes

The coordinates and the structure factors have been deposited in the RCSB Protein Data Bank with accession code **2YXV** (Δα5–7 CueO) and **2YXW** (Cu-soaked Δα5–7 CueO).

Acknowledgements

Financial supports from Nagase Science and Technology Foundation (to K. Kataoka), NEDO (to K. Kano), Toyota Motor Corporation (to K. Kano and T. Sakurai), the Foundation of University of Hyogo (to H. Komori), the Hyogo-ken Science Foundation (to H. Komori), the Yamanouchi Foundation for Research on Metabolic Disorders (to H. Komori), the Inamori Foundation (to H. Komori), the Japanese Aerospace Exploration Agency Project (to Y. Higuchi), and Grants-in-Aid for Scientific Research from the Ministry of Education, Science, Culture, and Sports, Japan (18770093 to H. Komori, 16074214 and 18GS0207 to Y. Higuchi, and 19350081 to T. Sakurai) and MANDOM Corporation (to T. Sakurai) are greatly acknowledged.

Supplementary Data

Supplementary data associated with this article can be found in the online version, at XXXXXXXX.

References

1 Messerschmidt, A. (ed) (1997) *Multi-copper oxidases*, World Scientific, Singapore.

2 Solomon, E. I., Sundaram, U. M. & Machonkin, T. E. (1996). Multicopper oxidases and oxygenases, *Chem. Rev.* **96**, 2563-2605.

3 Baldrian, P. (2006). Fungal laccases - occurrence and properties, *FEMS Microbiol. Rev.* **30**, 215-242.

4 Kataoka, K., Kitagawa, R., Inoue, M., Naruse, D., Sakurai, T. & Huang, H. W. (2005). Point mutations at the type I Cu ligands, Cys457 and Met467, and at the putative proton donor, Asp105, in *Myrothecium verrucaria* bilirubin oxidase and reactions with dioxygen, *Biochemistry* **44**, 7004-7012.

5 Quintanar, L., Stoj, C., Wang, T. P., Kosman, D. J. & Solomon, E. I. (2005). Role of aspartate 94 in the decay of the peroxide intermediate in the multicopper oxidase Fet3p, *Biochemistry* **44**, 6081-6091.

6 Leonowicz, A., Cho, N. S., Luterek, J., Wilkolazka, A., Wojtas-Wasilewska, M., Matuszewska, A., Hofrichter, M., Wesenberg, D. & Rogalski, J. (2001). Fungal laccase: properties and activity on lignin, *J. Basic Microbiol.* **41**, 185–227.

7 Bajpai, P. (1999). Application of enzymes in the pulp and paper industry, *Biotechnol. Prog.* **15**, 147-157.

8 Claus, H., Faber, G. & König, H. (2002). Redox-mediated decolorization of

synthetic dyes by fungal laccases, *Appl. Microbiol. Biotechnol.* **59**, 672-678.

9 Galante, Y. M. & Formantici, C. (2003). Enzyme applications in detergency and in manufacturing industries, *Curr. Org. Chem.* **7**, 1399–1422.

10 Pointing S. B. (2001). Feasibility of bioremediation by white-rot fungi, *Appl. Microbiol. Biotechnol.* **57**, 20–33.

11 Kim, C., Lorenz, W. W., Hoopes, J. T. & Dean, J. F. (2001). Oxidation of phenolate siderophores by the multicopper oxidase encoded by the *Escherichia coli* yacK gene, *J. Bacteriol.* **183**, 4866-4875.

12 Grass, G. & Rensing, C. (2001). CueO is a multi-copper oxidase that confers copper tolerance in *Escherichia coli*, *Biochem. Biophys. Res. Commun.* **286**, 902-908.

13 Ueki, Y., Inoue, M., Kurose, S., Kataoka, K. & Sakurai, T. (2006). Mutations at Asp112 adjacent to the trinuclear Cu center in CueO as the proton donor in the four-electron reduction of dioxygen, *FEBS Lett.* **580**, 4069-4072.

14 Martins, L. O., Soares, C. M., Pereira, M. M., Teixeira, M., Costa, T., Jones, G. H. & Henriques, A. O. (2002). Molecular and biochemical characterization of a highly stable bacterial laccase that occurs as a structural component of the *Bacillus subtilis* endospore coat, *J. Biol. Chem.* **277**, 18849-18859.

15 Durão, P., Bento, I., Fernandes, A. T., Melo, E. P., Lindley, P. F. & Martins, L. O. (2006). Perturbations of the T1 copper site in the CotA laccase from *Bacillus subtilis*: structural, biochemical, enzymatic and stability studies, *J. Biol. Inorg. Chem.* **11**, 514-526.

16 Rensing, C. & Grass, G. (2003). *Escherichia coli* mechanisms of copper homeostasis in a changing environment, *FEMS Microbiol. Rev.* **27**, 197-213.

17 Singh, S. K., Grass, G., Rensing, C. & Montfort, W. R. (2004). Cuprous oxidase activity of CueO from *Escherichia coli*, *J. Bacteriol.* **186**, 7815-7817.

18 Grass, G., Thakali, K., Klebba, P. E., Thieme, D., Müller, A., Wildner, G. F. & Rensing, C. (2004). Linkage between catecholate siderophores and the multicopper oxidase CueO in *Escherichia coli*, *J. Bacteriol.* **186**, 5826-5833.

19 Messerschmidt, A., Ladenstein, R., Huber, R., Bolognesi, M., Avigliano, L, Petruzzelli, R., Rossi, A. & Finazzi-Agró, A. (1992). Refined crystal structure of ascorbate oxidase at 1.9 Å resolution, *J. Mol. Biol.* 224, 179-205.

20 Bento, I., Peixoto, C., Zaitsev, V. N. & Lindley, P. F. (2007). Ceruloplasmin revised: structural and functional roles of various metal cation-binding sites, *Acta Crystallogr. Sect. D* **63**, 240-248.

21 Ducros, V., Brzozowski, A. M., Wilson, K. S., Ostergaard, P., Schneider, P., Svendson, A. & Davies, G. J. (2001). Structure of the laccase from *Coprinus cinereus* at 1.68 Å resolution: evidence for different 'type 2 Cu-depleted'

isoforms, *Acta Crystallog. Sect. D* **57**, 333-336.

22 Bertrand, T., Jolivalt, C., Briozzo, P., Caminade, E., Joly, N., Madzak, C. & Mougin, C. (2002). Crystal structure of a four-copper laccase complexed with an arylamine: insights into substrate recognition and correlation with kinetics, *Biochemistry* **41**, 7325-7333.

23 Piontek, K., Antorini, M. & Choinowski, T. (2002). Crystal structure of a laccase from the fungus *Trametes versicolor* at 1.90-Å resolution containing a full complement of coppers, *J. Biol. Chem.* **277**, 37663-37669.

24 Antorini, M., Herpoël-Gimbert, I., Choinowski, T., Sigoillot, J. C., Asther, M., Winterhalter, K. & Piontek, K. (2002). Purification, crystallisation and X-ray diffraction study of fully functional laccases from two ligninolytic fungi, *Biochim. Biophys. Acta* **1594**, 109-114.

25 Hakulinen, N., Kiiskinen, L. L., Kruus, K., Saloheimo, M., Paananen, A., Koivula, A. & Rouvinen, J. (2002). Crystal structure of a laccase from *Melanocarpus albomyces* with an intact trinuclear copper site, *Nat. Struct. Biol.* **9**, 601-605.

26 Garavaglia, S., Cambria, M. T., Miglio, M., Ragusa, S., Iacobazzi, V., Palmieri, F., D'Ambrosio, C., Scaloni, A. & Rizzi, M. (2004). The structure of *Rigidoporus lignosus* laccase containing a full complement of copper ions, reveals an asymmetrical arrangement for the T3 copper pair, *J. Mol. Biol.* **342**, 1519-1531.

27 Taylor, A. B., Stoj, C. S., Ziegler, L., Kosman, D. J. & Hart, P. J. (2005) The copper-iron connection in biology: structure of the metallo-oxidase Fet3p, *Proc. Natl. Acad. Sci. U. S. A.* 102, 15459-15464.

28 Roberts, S. A., Weichsel, A., Grass, G., Thakali, K., Hazzard, J. T., Tollin, G., Rensing, C. & Montfort, W. R. (2002). Crystal structure and electron transfer kinetics of CueO, a multicopper oxidase required for copper homeostasis in *Escherichia coli*, *Proc. Natl. Acad. Sci. U. S. A.* **99**, 2766-2771.

29 Enguita, F. J., Martins, L. O., Henriques, A. O. & Carrondo, M. A. (2003). Crystal structure of a bacterial endospore coat component. A laccase with enhanced thermostability properties, *J. Biol. Chem.* **278**, 19416-19425.

30 Smith, A. W., Camara-Artigas, A., Wang, M., Allen, J. P. & Francisco, W. A. (2006). Structure of phenoxazinone synthase from *Streptomyces antibioticus* reveals a new type 2 copper center, *Biochemistry* **45**, 4378-4387.

31 Murphy, M. E., Lindley, P. F. & Adman, E. T. (1997). Structural comparison of cupredoxin domains: domain recycling to construct proteins with novel functions, *Protein Sci.,* **6,** 761-770.

32 Nersissian, A. M. & Shipp, E. L. (2002). Blue copper-binding domains, *Adv. Prot.*

Chem. **60**, 271-340.

33 Roberts, S. A., Wildner, G. F., Grass, G., Weichsel, A., Ambrus, A., Rensing, C. & Montfort, W. R. (2003). A labile regulatory copper ion lies near the T1 copper site in the multicopper oxidase CueO, *J. Biol. Chem.* **278**, 31958-31963.

34 Kurose, S., Kataoka, K., Otsuka. K., Tsujino, Y. & Sakurai, T. (2007). Promotion of laccase activities of *Escherichia coli* cuprous oxidase, CueO by deleting the segment covering the substrate binding site, *Chem. Lett*. **36**, 232-233.

35 Li, X., Wei, Z., Zhang, M., Peng, X., Yu, G., Teng, M. & Gong, W. (2007) Crystal structure of *E. coli* at different copper concentrations, *Biochim. Biophys. Res. Commun*. **354**, 2126-2131.

36 Kukimoto, M., Nishiyama, M., Tanokura, M., Adman, E. T. & Horinouchi, S. (1996). Studies on protein-protein interaction between copper-containing nitrite reductase and pseudoazurin from *Alcaligenes faecalis* S-6, *J. Biol. Chem.* **271**, 13680-13683.

37 Kataoka, K., Yamaguchi, K., Kobayashi, M., Mori, T., Bokui, N. & Suzuki, S. (2004). Structure-based engineering of *Alcaligenes xylosoxidans* copper-containing nitrite reductase enhances intermolecular electron transfer reaction with pseudoazurin, *J. Biol. Chem.* **279**, 53374-53378.

38 Banci, L. & Rosata, A. (2003) Structural genomics of proteins involved in copper homeostasis, *Acc. Chem. Res.* **36**, 215-221.

39 Kataoka, K., Tanaka, K., Sakai, Y. & Sakurai, T. (2005) High-level expression of *Myrothecium verrucaria* bilirubin oxidase in Pichia pasatoris, and its facile purification and characterization, *Prot. Exp. Purif.* **41**, 77-83.

40 Nagai, M., Sato, T., Watanabe, H., Saito, K., Kawata, M. & Enei, H. (2002). Purification and characterization of an extracellular laccase from the edible mushroom *Lentinula edodes*, and decolorization of chemically different dues, *Appl. Microbiol. Biotechnol.* **60**, 327-335.

41 Kataoka, K., Furusawa, H., Takagi, K., Yamaguchi, Y. & Suzuki, S. (2000). Functional analysis of conserved aspartate and histidine residues located around the type 2 copper site of copper-containing nitrite reductase, *J. Biocem.* **127**, 345-350.

42 Higuchi, R. (1989) in *PCR Technology: Principles and Applications for DNA Amplification* (Erlich, H. A. ed) pp. 61-88, Stockton Press, New York.

43 Powell, H. R. (1999). The Rossmann Fourier autoindexing algorithm in MOSFLM. *Acta Crystallogr. Sect. D* **55**, 1690-1695.

44 Vagin, A. & Teplyakov, A. (2000). An approach to multi-copy search in molecular replacement. *Acta Crystallogr. Sect. D* **56**, 1622-1624.

45 Brunger, A. T., Adams, P. D., Clore, G. M., DeLano, W. L., Gros, P., Grosse-Kunstleve, R. W., Jiang, J. S., Kuszewski, J., Nilges, M., Pannu, N. S., Read, R. J., Rice, L. M., Simonson, T. & Warren, G. L. (1998). Crystallography & NMR system: A new software suite for macromolecular structure determination. *Acta Crystallogr. Sect. D* **54**, 905-921.

46 Emsley, P. & Cowtan, K. (2004). Coot: model-building tools for molecular graphics. *Acta Crystallogr. Sect. D* **60**, 2126-2132.

47 Winn, M. D., Isupov, M. N. & Murshudov, G. N. (2001). Use of TLS parameters to model anisotropic displacements in macromolecular refinement. *Acta Crystallogr D* **57**, 122-33.

48 Brunger, A. T. (1992). The free R value: a novel statistical quantity for assessing the accuracy of crystal structures. *Nature* **355**, 472-474.

49 Morris, A. L., MacArthur, M. W., Hutchinson, E. G. & Thornton, J. M. (1992). Stereochemical quality of protein structure coordinates. *Proteins* **12**, 345-364.

50 DeLano, W. L. (2002). in *The PyMOL Molecular Graphics System*, DeLano Scientific, San Carlos, CA, USA. http://www.pymol.org.

51 Kraulis , P. J. (1991). MOLSCRIPT: A program package to produce both detailed and schematic plots of protein structures . *J. Appl. Crystallogr.* **24**, 946-950.

52 Merrit, E. A. & Murphy, M. E. (1994). Raster3D Version 2.0: A program for photorealistic molecular graphics. *Acta Crystallogr. Sect. D* **50**, 869-873.

Figure Legends

Figure 1. The structure of CueO and folding topology of domain 3. (A) Ribbon diagram of CueO. Domain 3 of CueO is shown in blue and red colors (the anti-parallel connections of the first and second β-strands of domain 3 are highlighted in green). The region between α–helix 5 and α–helix 6 (broken line) is not seen because of high mobility. To generate the Δα5-7 deletion mutant, the amino acid residues in the α-helical region from Pro357 to His406 (red colored) were deleted, and replaced by the dipeptide Gly-Gly. Red, blue, green, and orange spheres indicate the labile (regulatory) Cu

(rCu), type I Cu, type II Cu, and type III Cu ions, respectively. The figure was drawn with PyMOL[50] using the coordinates from PDB file 1N68. (B) Schematic diagram of the β-barrel structure of domain 3. The domain made up of two five-stranded β-sheets (one additional strand is inserted in each sheet) forms the β-sandwich structure. The structurally unconserved regions (SURs) are illustrated by wire. The color scheme is as in (A).

Figure 2 Superposition of the Cα atoms of Δα5-7 CueO (blue) and rCueO (red).

Figure 3 Overall structure of Δα5-7 CueO (Molecule A). Domain 1 is colored pale pink, domain 2 pale green, and domain 3 pale blue. Type I Cu, type II Cu and type III Cu's are depicted as blue sphere, green sphere and orange spheres, respectively.

Figure 4. Superposition of the Cu-binding sites of Δα5−7 CueO onto those of rCueO. Δα5−7 CueO is shown as atomic color coding and green, and rCueO in pale atomic coding. Type I Cu, type II Cu, type III Cu and rCu are shown as blue sphere, green sphere, orange sphere, and red sphere, respectively. Met355, Asp439 and Met441 are the rCu ligands and Asp360 is deleted in Δα5−7 CueO. Asp112 is the putative proton donor. Type I Cu is ligated by His443, Cys500, His505, and Met510. Type II Cu is ligated by His101, His446, and a water molecule. One type III Cu is ligated by His103, His141, and His501 and the other type III Cu by His143, His448, and His 499. An OH^- ion (oxygen atom figures as a small pale blue sphere) bridges between type III Cu's.

Figure 5. Electronic absorption (A, top), CD (A, bottom), and EPR spectra (B) of rCueO (dotted line) and Δα5-7 CueO (solid line). Measurement conditions: (A) 0.1 M potassium phosphate buffer (pH 6.0) at room temperature; (B) 0.1 M potassium phosphate buffer (pH 6.0) at 77 K; microwave frequency, 9.20 GHz; microwave power, 5 mW; modulation frequency, 100 kHz; modulation amplitude, 1 mT; filter, 0.1 s; sweep time, 4 min; amplitude, 400.

Figure 6. Cyclic voltammograms of rCueO (dotted line) and Δα5-7 CueO (solid line). The background for Δα5-7 CueO is subtracted. The working electrode is a gold disk modified with thioglycolate. Measurement conditions: 0.1 M potassium phosphate buffer (pH 6.0) at room temperature; protein concentrations, 51 μM; scan rate, 2 $mV \cdot s^{-1}$.

Table 1. X-ray crystallographic data

	Data 1	Data 2 (Cu-soaked)	Data 3 (Cu-soaked)
Source	RA-Micro7	SPring BL38B	SPring BL38B
Wavelength (Å)	1.542	1.000	1.378
Space group	P_1	P_1	
Cell constants			
a, *b*, *c* (Å)	49.98, 50.95, 86.05	50.33, 51.57, 86.70	
α, β, γ (°)	83.2, 90.8, 66.7	83.8, 90.4, 67.1	
Resolution (Å)	30.0-1.81 (1.90-1.81)	30.0-1.5(1.55 -1.50)	30.0-2.27(2.37-2.27)
Completeness (%)	92.1 (85.8)	95.2 (94.7)	90.51 (88.6)
Redundancy	2.0	2.0	2.0
I/σ(I)	14.1 (3.0)	35.0 (6.6)	32.6 (27.5)
*R*merge (%)	5.5 (31.2)	3.4 (9.7)	3.2 (4.6)
R-value (%)	17.2 (17.8)	18.0 (22.3)	
R-free (%)	20.8 (22.3)	20.8 (24.1)	
No. of reflections	65489 (2118)	1271073 (2118)	
No. of protein atoms	6768	6772	
No. of hetero atoms	14	16	
No. of water oxygen atoms	394	658	

Table 2. Copper-ligand distances and angles

	Δα5-7 CueO (A)	Δα5-7 CueO (B)	rCueO (**1KV7**)[28]
Type I Cu			
Cu(1)-His443 (Å)	2.04	2.01	2.02
Cu(1)-Cys500 (Å)	2.15	2.20	2.19
Cu(1)-His505 (Å)	1.99	1.99	1.98
Cu(1)-Met510 (Å)	3.28	3.38	3.23
Type II Cu			
Cu(4)-His101 (Å)	1.98	1.99	1.92
Cu(4)-His446 (Å)	1.96	1.93	1.83
Cu(4)-HOH (Å)	2.49	2.52	2.96
Type III Cu			
Cu(2)-O (Å)	1.97	1.95	2.29
Cu(2)-His143 (Å)	2.02	2.05	2.02
Cu(2)-His448 (Å)	2.03	2.07	1.94
Cu(2)-His499 (Å)	2.04	2.05	2.02
Cu(3)-O (Å)	1.96	1.96	2.43
Cu(3)-His141 (Å)	2.10	2.05	1.97
Cu(3)-His103 (Å)	2.13	2.04	1.96
Cu(3)-His501 (Å)	2.02	2.04	2.09
Cu(2)-Cu(3) (Å)	3.79	3.75	4.70
Cu(2)-Cu(4) (Å)	3.48	3.47	3.54
Cu(3)-Cu(4) (Å)	3.89	3.87	3.98
Cu(2)-O-Cu(3) Angle (°)	149.8	146.9	169.3

Table 3. Substrate specificities of rCueO and Δα5-7 CueO

Substrate (mM)	Activity (U/mg)[a]			
	rCueO		Δα5-7 CueO	
	Without Cu	1 mM Cu[b]	Without Cu	10 mM Cu[c]
Cu(I) (0.10)[d]	187	201	21	24

Fe(II) (0.5)	0.91	53	0.70	43
ABTS (6.0)	0.45	16	15	34
p-PD (5.0)	0.53	19	4.6	20[e]
2,6-DMP (10.0)	0	29	0	30
Catechol (3.0)	0	12	0	52
Guaiacol (10.0)	0	0	0	5.5
Syringaldazine (0.01)	0	0	0.11	0.29

[a] One unit is the amount of enzyme that oxidizes 1 μmol of substrate per min in 0.1 M acetate buffer (pH 5.5) at 25°C.

[b] The activity was measured in the presence of 1 mM $CuSO_4$.

[c] The activity was measured in the presence of 10 mM $CuSO_4$.

[d] The activity was measured with an oxygen electrode as described in Materials and Methods.

[e] The activity was inhibited by high concentrations of Cu(II) because of complex formation between *p*-PD and Cu(II), and was measured in the presence of 1 mM $CuSO_4$. The activity in the presence of 10 mM $CuSO_4$ was 4.7 U/mg.

Table 4. Kinetic constants of rCueO and Δα5-7 CueO for ABTS, *p*-PD, and 2,6-DMP in the presence and absence of Cu(II) ions.

Substrate	Cu(II)[a]	rCueO		Δα5-7 CueO	
		K_m (mM)	V_{max} (U/mg)	K_m (mM)	V_{max} (U/mg)
ABTS	-	6.5 ± 0.3	1.1 ± 0.1	12 ± 1	46 ± 1
	+	6.4 ± 0.3	34 ± 1	11 ± 0.1	39 ± 1
p-PD	-	375 ± 93	55 ± 11	90 ± 9	108 ± 4
	+	ND[b]	ND[b]	ND[b]	ND[b]
2,6-DMP	-	ND[c]	~0	ND[c]	~0
	+	2.5 ± 0.1	48 ± 1	1.8 ± 0.1	35 ± 1

[a] Plus (+) indicates that 1 mM $CuSO_4$ (for rCueO) or 10 mM $CuSO_4$ (for Δα5-7 CueO) was added to the reaction mixture and minus (-) indicates that $CuSO_4$ was not added.

[b] Not determined due to complex formation between Cu(II) and *p*-PD.

[c] Not determined due to low activity with 2,6-DMP.

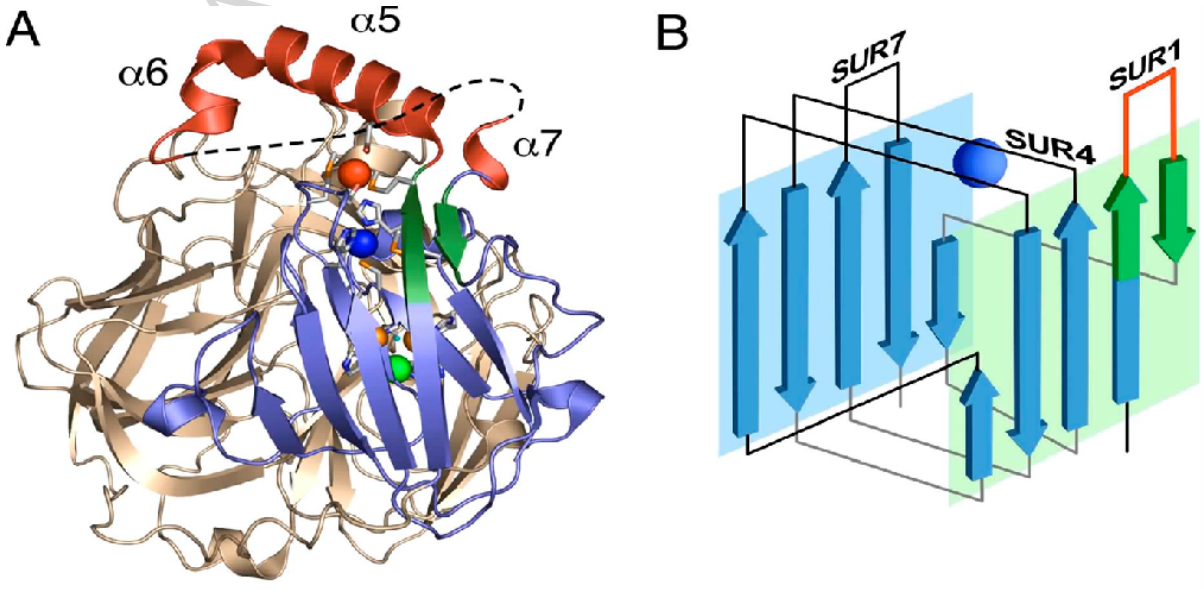

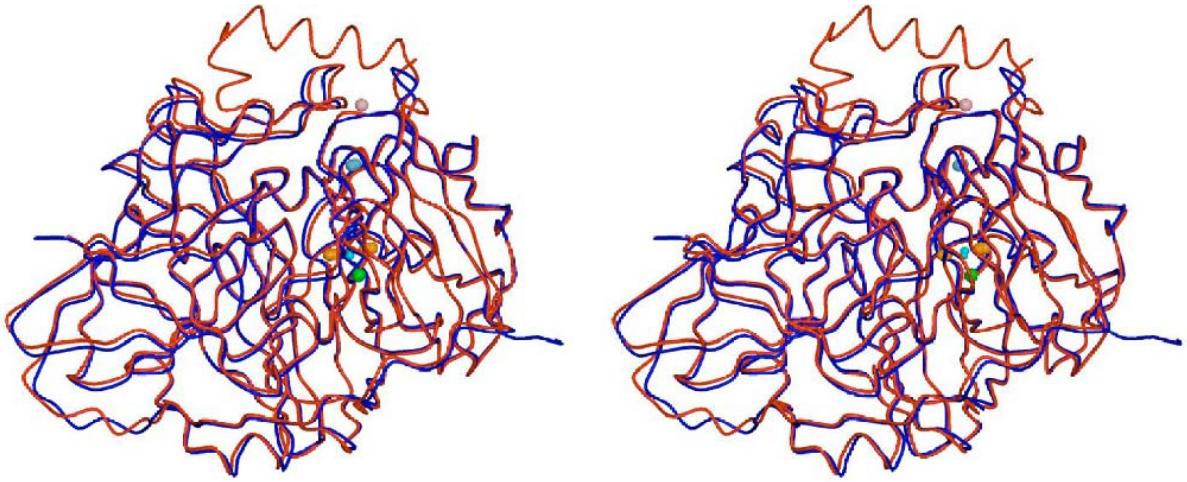

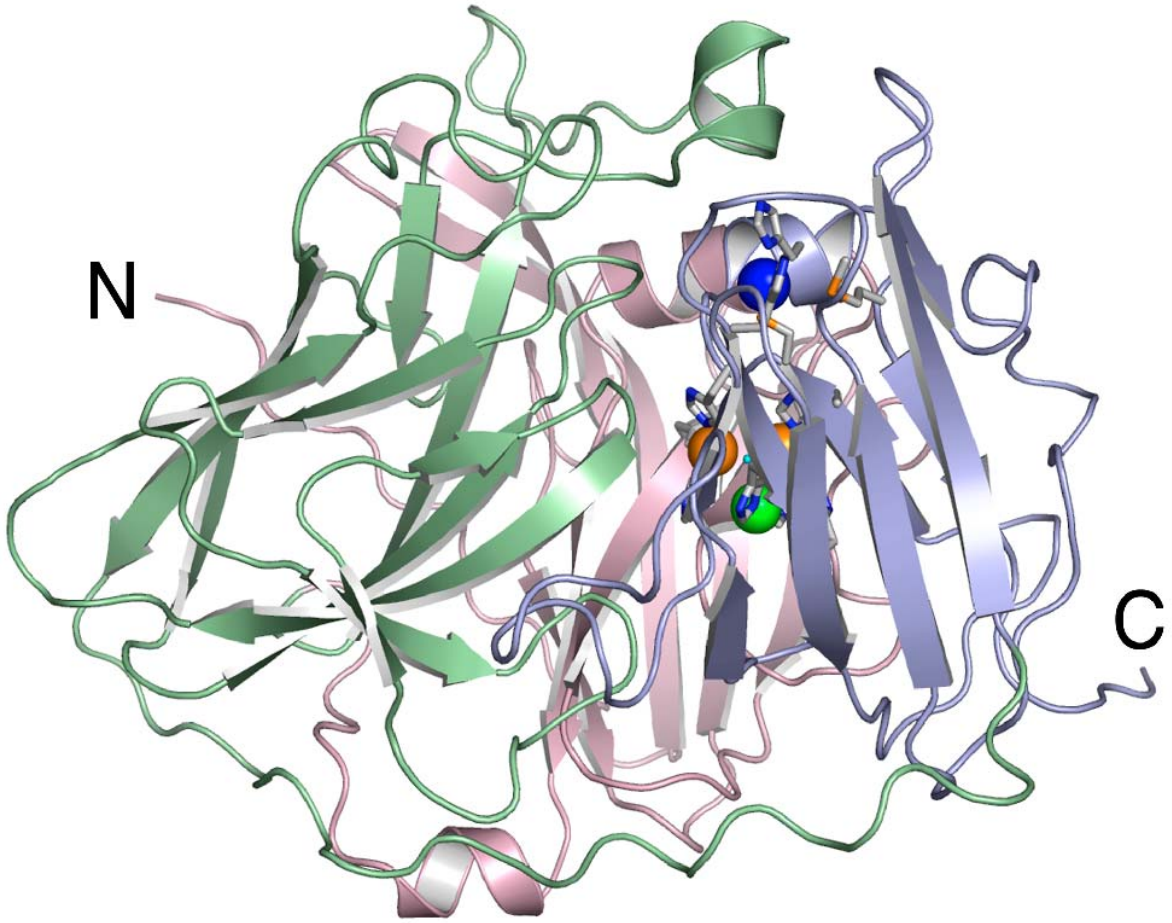

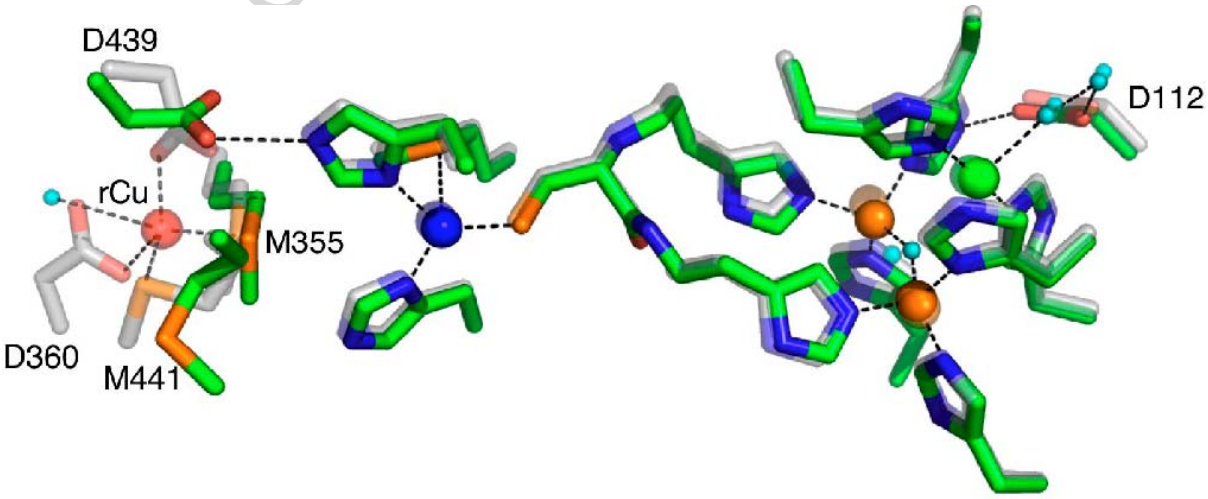

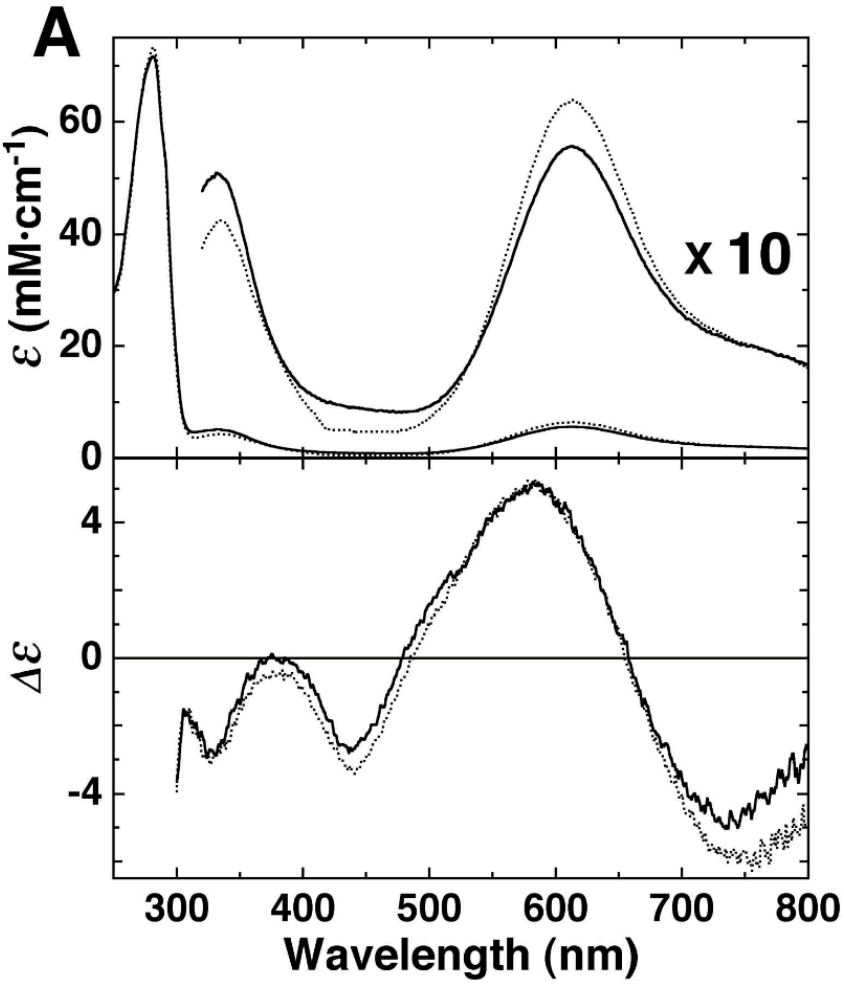
A
ε (mM·cm⁻¹)
60
40
20
0
x 10
4
0
-4
Δε
300
400
500
600
700
800
Wavelength (nm)

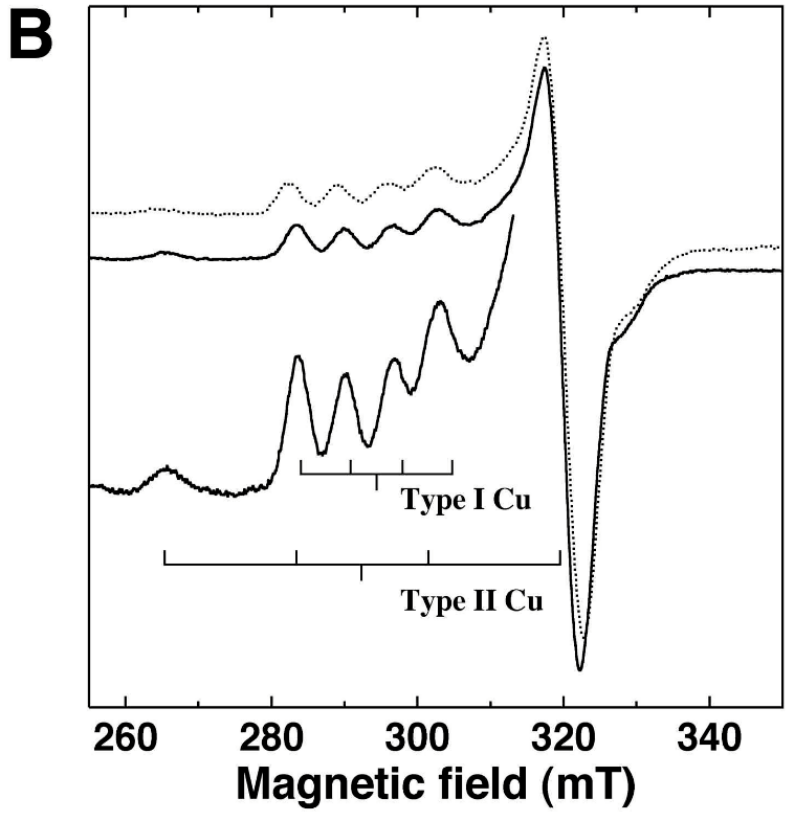
B
Type I Cu
Type II Cu
260
280
300
320
340
Magnetic field (mT)